processes

MDPI

*Article*

# Field Investigation and Stability Analysis of Gob-Side Roadway Retention with an 8 m Coal Pillar in Extra-Thick Coal Seam Mining

**Tao Ding [1], Wei Wang [2], Chunwang Zhang [1,3,*], Wenyang Zhang [4,*] and Yulong Chen [5]**

[1] Anhui Wanbei Coal-Electricity Group Co., Ltd., Suzhou 234000, China; anhuidingtao@126.com
[2] Jiaojiazai Coal Mine, Datong Coal Mine Group Xuangang Coal-Electric Co., Ltd., Xinzhou 034115, China; wangwei@163.com
[3] College of Safety and Emergency Management Engineering, Taiyuan University of Technology, Taiyuan 030024, China
[4] Jinneng Holding Shanxi Science and Technology Research Institute Co., Ltd., Taiyuan 030032, China
[5] Shanxi Coal Transportation and Sales Group Science and Technology Research Co., Ltd., Taiyuan 030006, China; chenyulong@163.com
* Correspondence: zhangchunwang@tyut.edu.cn (C.Z.); zhangwenyang1986@163.com (W.Z.)

**Abstract**

To improve the stability of gob-side entry in the mining of extra-thick coal seams, we examined the field practice of reserving a narrow coal pillar with a width of 8 m in a 17 m thick coal seam. A combination of roof directional hydraulic fracturing and pouring concrete to consolidate the coal pillars was proposed and applied to reduce the deformation of the gob entry. First, roof directional hydraulic fracturing inhibits the vertical stress transmission to the key roof strata, and it transfers more vertical stress to the gob and reduces the lateral abutment stress in the roof. Subsequently, the narrow coal pillar is strengthened with a reinforced concrete wall, forming a strong–weak coupled bearing structure capable of bearing the overburden load, and the higher stiffness of the reinforced concrete wall effectively resists the lateral deformation of the coal pillar into the roadway. Additionally, the feasibility of this application was verified by comparing the results with the roadway convergence for a 43 m coal pillar on site. The results show that the maximum convergence, stability time, and advanced influence range were all significantly decreased by the proposed method, and the gob-side entry stability was improved. The proposed method and the results obtained provide a valuable reference for mining in similar conditions.

**Keywords:** extra-thick coal seam; narrow coal pillar; gob-side entry stability; directional hydraulic fracturing; in situ application

Check for updates

Academic Editor: Wei Liu

Received: 15 May 2026
Revised: 17 June 2026
Accepted: 26 June 2026
Published: 4 July 2026

**Copyright:** © 2026 by the authors. Licensee MDPI, Basel, Switzerland. This article is an open access article distributed under the terms and conditions of the Creative Commons Attribution (CC BY) license.

## 1. Introduction

During underground mining, the regional geo-stress is redistributed, and the overburden strata break and move [1–4]. To ensure the safety of the workspace, coal pillars with different widths are widely used to support the roof. For example, in the chamber-and-pillar method, the sizes of the coal houses and coal pillars are usually maintained in an appropriate proportion to ensure safe mining [5,6]. In the strip-mining method, coal pillars of a reasonable size are beneficial in controlling land subsidence [7–9]. Recently, with the improvement in machine mining, fully mechanized longwall mining technology has become the most important way to achieve efficient, high-production mining [10,11].

Generally, the protecting coal pillars are reserved between two adjacent working faces to maintain the roadway stability [12,13]. However, the positions of the roadway and the adjacent coal pillars are usually determined during the coal mining design, and an unreasonable arrangement will cause deformation during the roadway excavation and mining process (Figure 1). Therefore, the deformation of the coal pillars under disturbed loads directly determines the stability of the roadway.

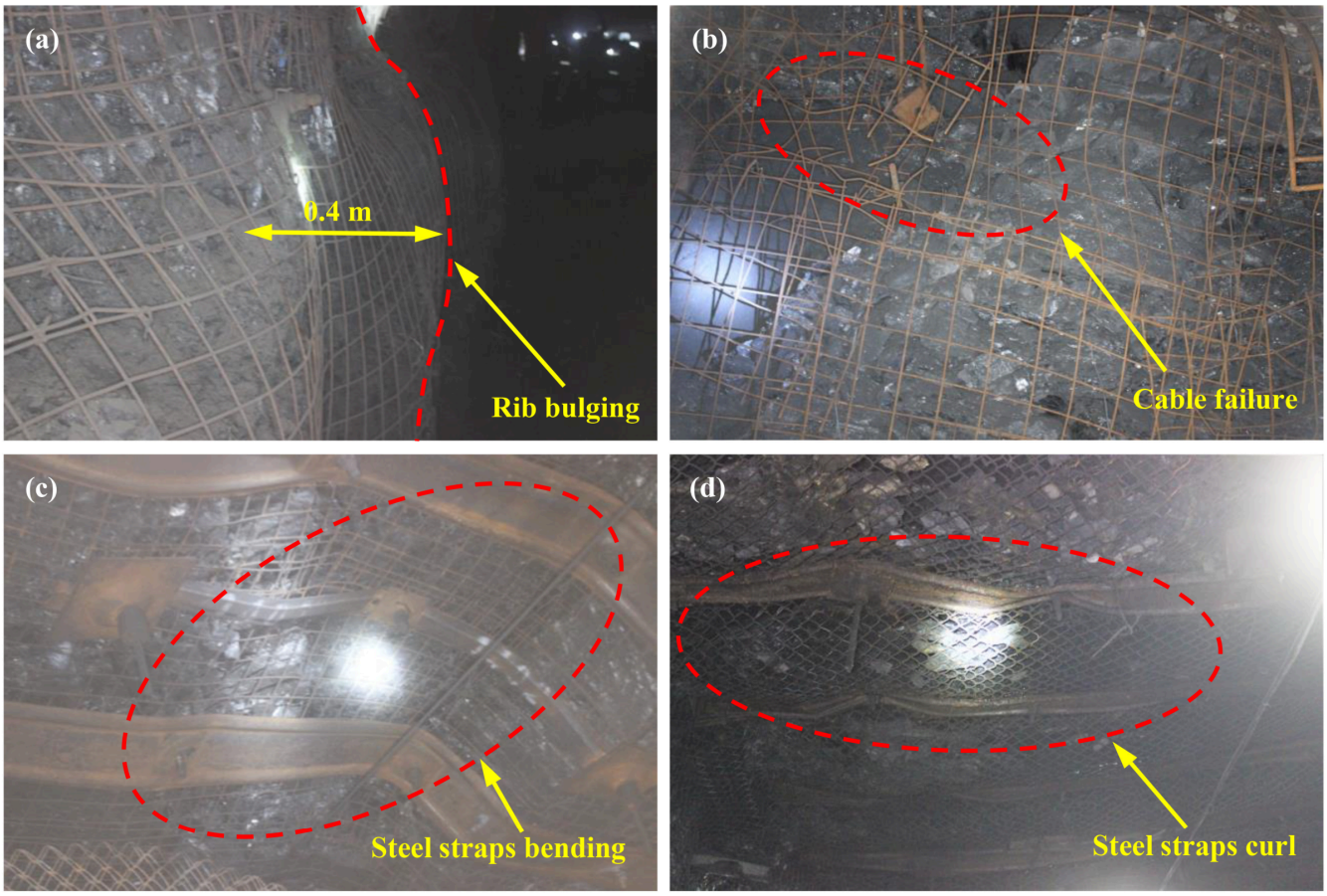



**Figure 1.** Roadway deformation: (**a**) rib bulging; (**b**) cable failure; (**c**) roof deflection; (**d**) fractured roof.

Understanding coal pillar stability and its potential impact on the adjacent roadway is the goal of all major mining engineers worldwide [14,15]. Over the last decade, based on the behavior of overburden strata breaking and coal pillar mechanics [16,17], various methods have been adopted to investigate the relationship between the reserved coal pillars and the adjacent roadway. These methods include in situ tests [18–20], theoretical analysis [21,22], experimental investigations [23,24], and numerical simulations [25,26]. These studies have shown that the size and bearing capacity of the protecting coal pillar play a critical role in gob-side entry stability. Bai et al. explored the progressive failure characteristics and surrounding fracture evolution of a water-rich roof using discrete element modeling [27]. Wang et al. optimized the roadway position in a low-stress area and reported that the width of the segment pillar should be 5–7 m [28]. Li and Chai concluded that a coal pillar experiences four stages, from stable to yield, using field monitoring and numerical simulations [29]. Wu et al. investigated the destruction process of a 7 m wide gob-side coal pillar and reported that the deformation was approximately 1.5 m when the pillar yielded [30]. Zhang et al. conducted field research on the ground response of 17 m thick coal seam mining, and they concluded that a 30 m wide coal pillar could be reduced [31]. Recently, the application of innovative technologies such as hydraulic fracturing [32,33],

pre-split blasting [34,35] and no-pillar mining technology [36–38] has been implemented in medium-thickness coal seams. Wu et al. inquired into the failure mechanism of roadside backfill bodies [39]. Wang et al. introduced the no-pillar technique and successfully performed it in longwall mining [40]. Yang et al. proposed a novel method of combined deep hole blasting to protect the gob-side roadway from dynamic disasters [41]. Lv et al. investigated the response characteristics of roadway-surrounding rock under multi-factor dynamic loading [42]. Zhang et al. explored the remnant pillar failure mechanism to determine a reasonable location of the lower coal seam entry [43]. Qiu et al. pointed out that concentrated stress from dredging is key to preventing rock burst hazards in deep coal mines [44]. Xia et al. studied the dynamic evolution characteristics of the 6.0 m coal pillar vertical stress and plastic state using a numerical simulation model [45]. Meng et al. presented a combined support measure of "roof cutting + roof support above RBBs + RBB reinforcement" to prevent shear fracture propagation [46]. In summary, the size of the coal pillars has a relation to various factors, such as geological conditions, lithology of surrounding rocks, the mining method used, mining depth, and coal seam thickness.

In high coal seam and ultra-thick coal seam mining, the mechanical behavior of the overburden strata is more intense, and the roadway deformation becomes more severe [47–49]. At this time, a larger coal pillar needs to be reserved to bear the roof weighting and increase the safety of the adjacent roadway. For example, 30 m coal pillars are usually reserved for 11 m high coal seam mining in Xinjiang, China. In the Datong ore district, the coal pillars are usually 35–45 m thick in 20–30 m ultra-thick coal seam mining. However, the on-site results of the larger coal pillars were not as good as expected. The comprehensive field studies that Chen et al. [50] and Zhang et al. [51] conducted in a thick coal seam mine also confirmed this phenomenon. In addition, the larger protecting coal pillars not only increase the cost of restoration but also waste a lot of coal resources [52]. Therefore, the traditional methods of stabilizing coal seams should be altered, and an innovative design should be created. Thus, we propose an innovative narrow coal pillar mining technique combined with directional hydraulic fracturing and pouring concrete to consolidate the coal pillars, and then, we implement the use of an 8 m wide protecting coal pillar in the longwall mining of extra-thick coal seams in the Tashan coal mine, Datong, China. This application allowed us to determine whether the narrow 8 m wide coal pillar could bear the stress of multiple disturbances and control the deformation of the roadway. As is well known, the in situ practice comparison test is the most indispensable way to verify suitability. The actual measured results can be used to evaluate the roadway and the coal pillar's stability. Moreover, the results provide strong support for the optimum coal pillar size in future designs.

Previous studies have demonstrated the effectiveness of narrow coal pillars, directional hydraulic fracturing (DHF), and roadside reinforcement for controlling roadway deformation. However, most of these studies have focused on medium-thickness coal seams or have examined these techniques separately. In extra-thick coal seam mining, especially under fully mechanized top-coal caving conditions, the overlying strata movement is stronger, the mining-induced stress redistribution is more complex, and the stability of gob-side entries with narrow coal pillars is more difficult to maintain. Therefore, the combined use of DHF for roof pressure relief and reinforced concrete walls (RCWs) for coal-pillar-side reinforcement in extra-thick seam narrow pillar mining remains insufficiently investigated, particularly in terms of field performance and deformation control effects.

To address this gap, this study takes the top-coal caving mining of the #3–5 extra-thick coal seams in the Tashan coal mine as an engineering case. Field measurements were conducted to compare the roadway deformation characteristics under two different coal pillar widths, namely an 8 m narrow coal pillar and a 43 m wide coal pillar, during roadway

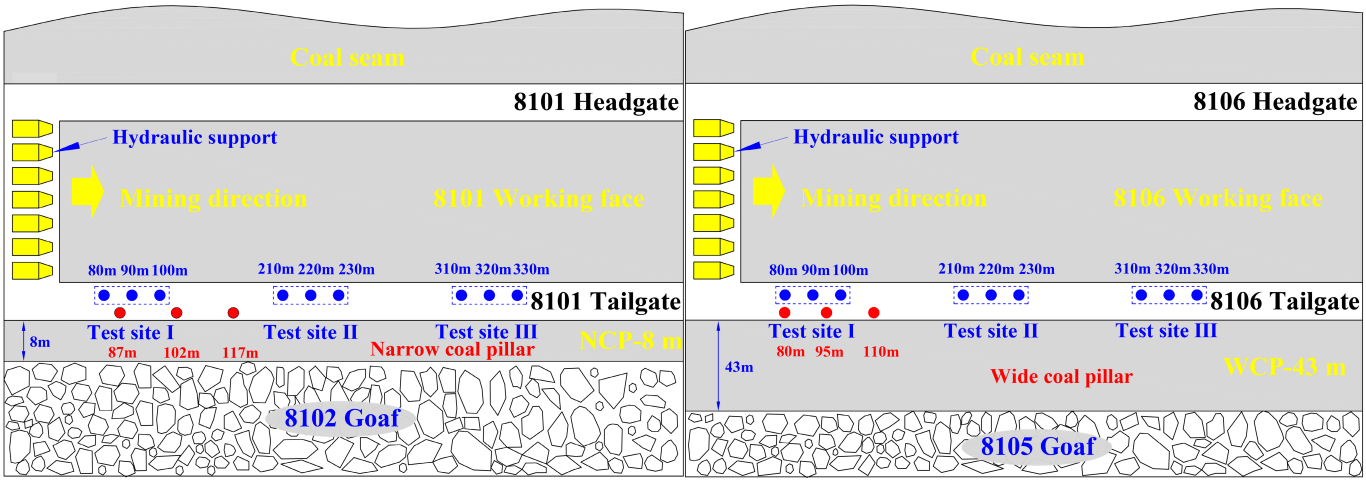
excavation and working face advancement. On this basis, an integrated control method combining roof directional hydraulic fracturing and reinforced concrete wall reinforcement was proposed and applied to the 8 m narrow coal pillar roadway. The novelty of this study lies in the field verification of the cooperative control effect of the NCP + DHF + RCW system in a 17 m thick extra-thick coal seam, where DHF is used to weaken roof stress transfer and the RCW is used to enhance the bearing capacity of the coal pillar side. The results provide practical evidence for reducing coal pillar width, improving resource recovery, and maintaining roadway stability in extra-thick coal seam mining.

## 2. Engineering Background

### *2.1. Mining Background and Monitoring Program*

The Tashan mining area is located in southwestern Datong County, Shanxi Province, China. The typical extra-thickness #3–5 coal seams (buried depth of 466 m) were formed in the Permo-Carboniferous period. Top-coal caving mining technology was adopted for mining coal, with a mining height and caving thickness of 3.5 m and 13.5 m, respectively. Many previous studies have presented an overview of the Tashan colliery [53] and have reported that the extra-thick coal seam reserves are abundant. The colliery's output can reach 30 million tons per year, given high-intensity mining. However, due to the huge space mined in the #3–5 extra-thick coal seams, the collapse of the overlying strata has caused severe deformation of the gob-side roadway due to support failure. Thus, an innovative design is needed to improve stability. In this section, we compare two working faces with different-sized coal pillars.

The selected experimental working faces are working face 8101 and working face 8106, which are located in the same panel and have similar initial conditions (Figure 2). The biggest difference between the two working faces is the size of the coal pillars adjacent to the goaf. According to the traditional design method, there is a 43 m wide coal pillar in working face 8106. However, coal pillars only 8 m wide were reserved in the narrow coal pillar technology test conducted on working face 8101. The strike length and dip length of workface 8101 are 1000 m and 230 m, and the strike length and dip length of workface 8106 are 1100 m and 210 m, respectively.




(**a**) Narrow coal pillar with 8 m (**b**) Traditional wide coal pillar with 43 m

**Figure 2.** Schematic diagram of the traditional, narrow mining method.

To verify the feasibility of the narrow coal pillar mining technique used on working face 8101, roadway convergence was monitored during roadway excavation and working face mining. During roadway excavation, three monitoring points (red dots in Figure 2)

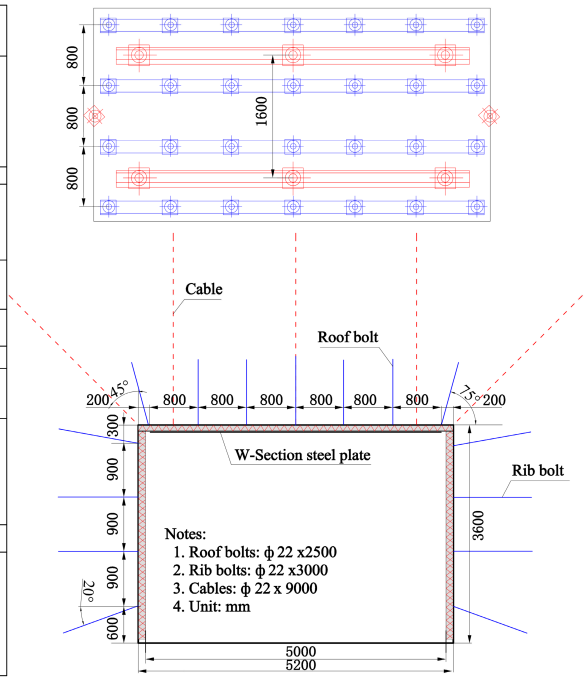
were arranged on the coal pillar side of the roadway of working faces 8101 and 8106. During coal face advancement, three monitoring regions and nine points (blue dots in Figure 2) were arranged on the roadway of working faces 8101 and 8106, respectively. The average distances from the three monitoring regions to the open-off cut were 90 m, 220 m, and 330 m. The roadway convergence was monitored using a YHJ40J laser distance-measuring instrument with an accuracy of 1 mm. To ensure data quality, all measuring instruments were calibrated prior to the field test. At each monitoring station, measurements were repeated three times, and the average value was calculated to represent the final convergence displacement. In addition, we also used borehole television to detect the extent of crack development in the narrow coal pillars.

### 2.2. Geological Conditions and Roadway Support Scheme

The simplified geological column of the #3–5 coal seams and a section of the roadway support design are shown in Figure 3. According to Qian's key strata classification theory [54], there are several key rock formation factors controlling the movement of the overburden strata. The roof immediately above the coal seam is gray mudstone (10.11 m), the main roof is composed of K3 medium sandstone (7.4 m), and the roof strata below the coal seam are gray mudstone (2.51 m) and coarse sandstone (20.85 m). Additionally, the roadway was excavated along the coal floor, with cross-sectional dimensions of 5.2 × 3.6 $m^2$. The support design and parameters are as follows.

| Depth (m) | Thickness (m) | Lithology | Description | Column |
|---|---|---|---|---|
| 410.31 | 20. 17 | Fine sandstone | Dark gray with plant rhizome fossils<br>Key stratum 2 | |
| 412.00 | 1.69 | No.4 coal seam | With 0-5 layers gangue | |
| 424.38 | 12.38 | Sandy mudstone | Dark grey with be'd'ding<br>Uniform partical size | |
| 431.78 | 7.40 | Medium sandstone | Compact and hard<br>Key stratum 1 | |
| 438.05 | 6.27 | Lamprophyre | Gray, uniform size, blocky | |
| 439.39 | 1.34 | No.2 coal seam | Black, contain gangue | |
| 449.50 | 10.11 | Mudstone | Dark carbonaceous mudstone<br>Blocky contain plant marks | |
| 465.72 | 16. 22 | 3-5# Coal | Semi-bright block structure with 2-16 layer gangue | |
| 396.96 | 2.51 | Mudstone | Gray-black, mainly kaolinite | |
| 416.07 | 20.85 | Coarse sandstone | Mainly quartz contain feldspar<br>Compact and crisp | |

(**a**) Geological column




(**b**) Traditional wide coal

**Figure 3.** Lithologic column and section of the roadway support design.

(1) Four anchors were used in each side of the roadway rib. The diameter and length of the bolts were 22 mm and 3000 mm, respectively, and the vertical and horizontal spacing of the bolts were 800 mm and 900 mm, respectively. In addition, a plastic mesh was installed over a 50 mm × 50 mm grid.

(2) Anchor and cable bolts were installed in the roof; anchors (22 mm in diameter and 2500 mm long) had vertical and horizontal spacings of 800 mm and 800 mm, respectively. The length and width of the arch anchor plate were both 150 mm, and the thickness of the anchor plate was 10 mm. Anchor cables (diameter of 22 mm and

length of 8300 mm) were installed vertically into the roof with horizontal spacings of 2000 mm and 1600 mm. The anchorage length was 1.5 m with a pre-tightening force of 170 kN, and a 6 mm thick JW steel belt was fixed at each cable's end.

(3) A single hydraulic prop was used to roof the fore poling. The support range was a 100 m advancement in the working face. A 1000 mm × 1200 mm roof cross-beam was placed on the four hydraulic props. The hydraulic prop was perpendicular to the roof.

## 3. Failure Mechanism and Key Techniques

As is well known, the overlying strata successively collapse and form a caving zone, a fractured zone, and a sagging zone [55,56]. At the same time, the abutment pressure accumulates in front of the working face, which shows a trend of increasing first and then decreasing to the original stress [57,58]. In the process of mining, the advanced fracture of the main roof will cause the coal pillar to enter the plastic state and reduce its bearing capacity. On the other hand, the articulated rock beam structure will bring greater lateral load pressure to the coal pillar beside the roadway. Furthermore, the size of a roadway located in an abutment stress environment is dependent on the size of the protecting coal pillar. Although the bearing capacity increases as the width of the coal pillar increases, it also results in the roadway being in the peak stress zone. As can be seen in Figure 4, if the width of the coal pillar increases further and the roadway is located in the original stress zone, a large amount of coal resources will be lost, and the recovery rate will decrease. Therefore, the roadway is placed in a relatively low-stress zone by reducing the width of the adjacent coal pillar. Extra-thick coal seam mining is often accompanied by larger collapse ranges and intense mining pressure, and these characteristics have a significant impact on narrow coal pillars. Thus, several technical measures are necessary to ensure that the mining is done safely.

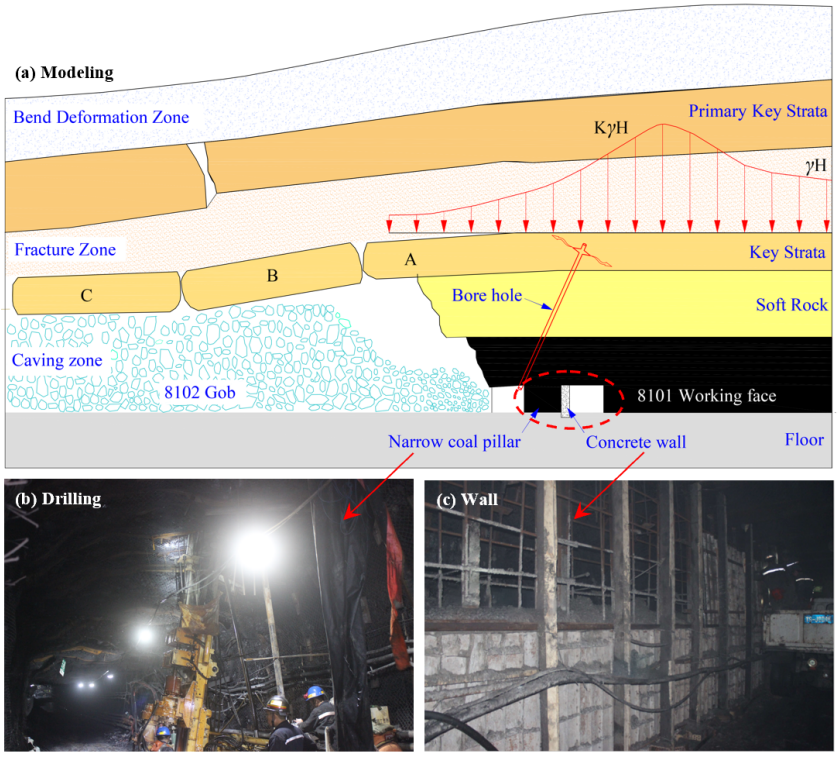



**Figure 4.** Roof directional hydraulic fracturing design and pouring concrete to consolidate the coal pillars.

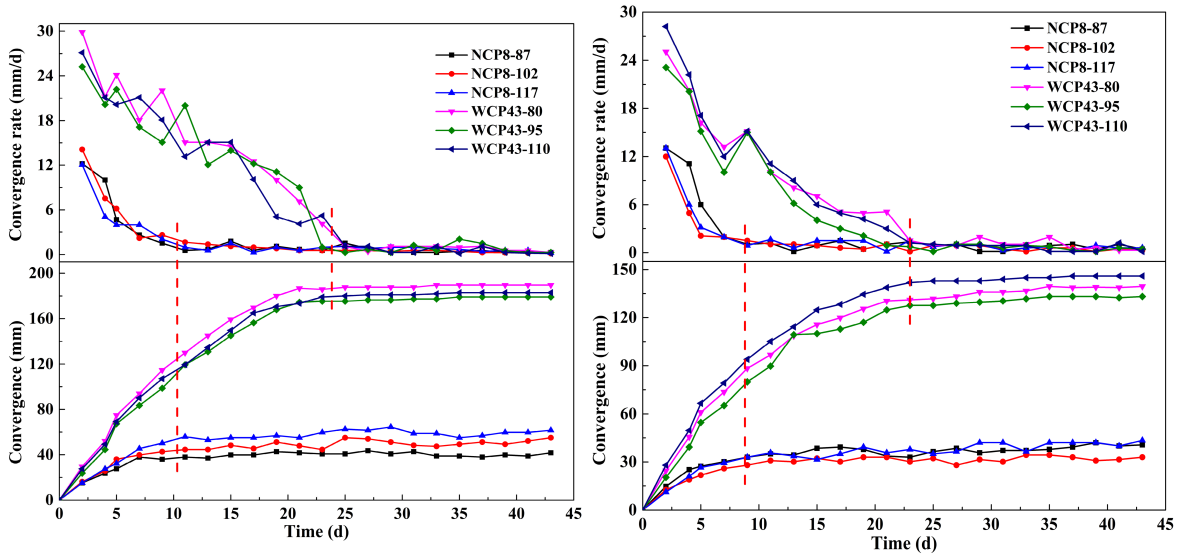
To improve the stability of the gob-side entry and the narrow coal pillars during mining, directional hydraulic fracturing was carried out on-site. As shown in Figure 4, a row of boreholes with a spacing of 20 m was arranged along the roadway. The diameter and depth of the holes were 54 mm and 35.5 m, respectively, and the angle between the drill borehole and the roof was 8° to ensure that the notched drilling bit would drill into the tight K3 sandstone formation. The drilling tool used to make the slots and the corresponding shape of the pre-notched crack are shown in Figure 4. By injecting high-pressure water into the hole, the rock surrounding the borehole was subjected to uniform compressive stress. When the pressure exceeded the rock's tensile strength, the crack extended further along the predefined direction. These cracks break the tight and intact rock strata, shorten the overhang distance, and weaken the roof weighting intensity on the coal pillar during mining.

To prevent the roadway rib on the coal pillar side from spalling off, a reinforced concrete wall was constructed in the roadway next to the narrow coal pillar before the working face was mined. As shown in Figure 4, the width and height of the reinforced concrete wall are 600 mm and 3600 mm, respectively. The bottom of the wall extends 50 mm into the coal seam floor, and the top of the wall abuts the roof of the roadway. The concrete used had a water: sand: cement (C42.5): gravel ratio of 1:2:3.5:6.8. The diameter and strength of the hot-rolled deformed bars were 22 mm and 400 MPa, respectively. It should be emphasized that the narrow coal pillar and the reinforced concrete wall do not exist in isolation, and they are tightly connected with cables to form a coal–concrete structure that allows them to bear the stress together. As the stiffness of concrete is much greater than that of coal, under the same vertical deformation conditions, the concrete can bear a larger overlying load and can restrain the coal pillar's lateral deformation. In addition, the reinforced concrete wall largely prevents the convex deformation of the gob-side entry.

## 4. Field Test Results and Analysis

### *4.1. Comparative Analysis of Roadway Deformation During Driving*

The deformation of tailgate 8101 and tailgate 8106 was monitored using field measurements. Figure 5 shows a comparison of the roadway convergence rate and the cumulative convergence for the use of narrow coal pillars (NCPs) and wide coal pillars (WCPs).



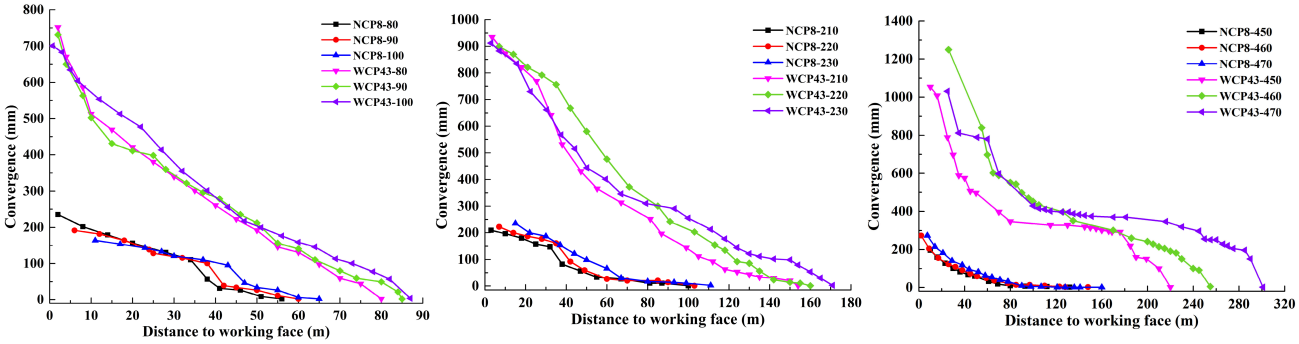

(**a**) Rib–to–rib deformation (**b**) Roof–to–floor deformation

**Figure 5.** Surrounding rock deformation measured during roadway driving in tailgate 8101 and tailgate 8106.

The collected deformation data can be summarized as follows: (1) As time passes, the deformation gradually stabilizes, and the roadway adjacent to the 8 m narrow coal pillar takes less time to stabilize than that adjacent to the 43 m wide coal pillar. The roadway stabilization times of the wide coal pillar and the narrow coal pillar are 23 d and 10 d, respectively. (2) The roadway convergence rate is high in the early stage, and then, it gradually decreases and becomes stable. The maximum convergence rates of the roadways with wide coal pillars and narrow coal pillars are 30 mm/d and 14 mm/d, respectively. (3) When the deformation is stable, the average maximum rib-to-rib convergences of the wide coal pillar and narrow coal pillar cases are 182 mm and 50 mm, respectively. The average maximum roof-to-floor convergences of the wide coal pillar and narrow coal pillar cases are 125 mm and 38 mm, respectively.

### *4.2. Comparative Analysis of Roadway Deformation During Mining*

As the working face is advanced, the gob-side entry is disturbed again due to mining-induced stress. A deformation comparison of the results for roadways with wide coal pillars and narrow coal pillars is shown in Figure 6.



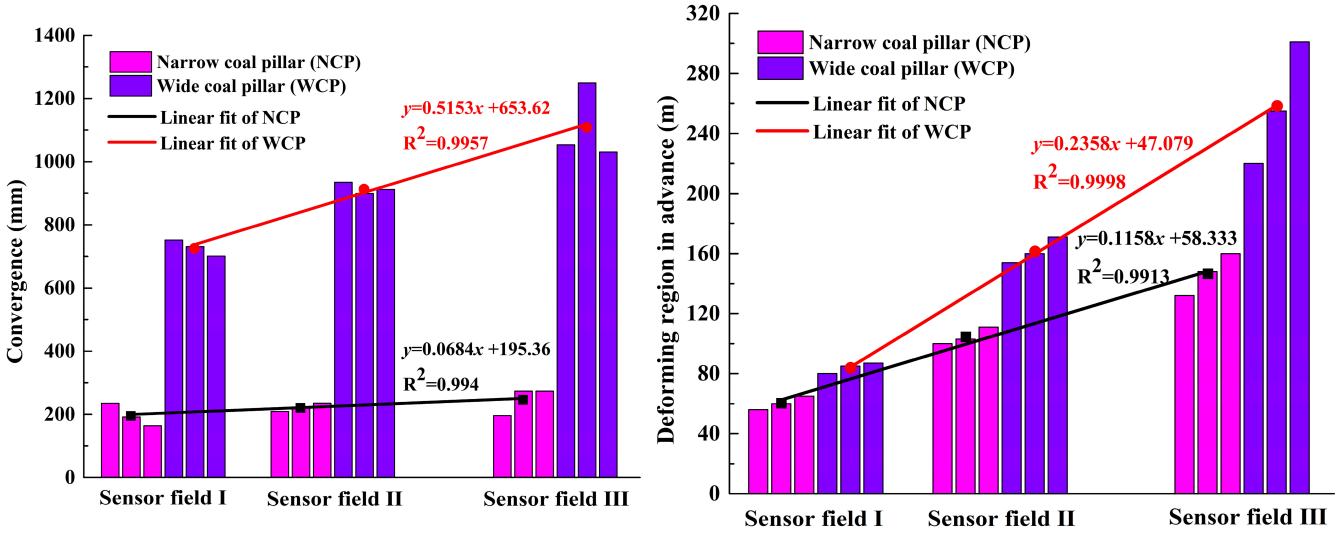

(**a**) Field test site I (**b**) Field test site II (**c**) Field test site III

**Figure 6.** Measured rib-to-rib deformation during the panel retreat in tailgate 8101 and tailgate 8106.

Figure 6 illustrates the rib-to-rib convergence as the longwall coal face approached the three monitoring sites. As the longwall working face was advanced, the entry convergences of both coal pillar cases increased gradually, and the cumulative convergence for the 43 m wide coal pillar was much greater than that for the 8 m narrow coal pillar. It should be noted that the convergence curves for the two different pillar sizes exhibit different growth patterns at different monitoring sites. As can be seen from the curves for the wide coal pillars at test site III (Figure 6c), the convergence curve shows an increase characteristic like that of a creep curve, which can be divided into three stages according to the slope rate: (1) In the initial phase, the initial convergence rate is higher, and then, it gradually decreases. (2) During the steady growth stage, the convergence increases at a relatively small constant rate. (3) In the accelerated increase phase, the rate of convergence gradually increases until the longwall panel reaches the monitoring site. However, the convergence of the narrow coal pillar remains stable in the long term and exhibits exponential growth characteristics. In addition, the convergence magnitudes and rates increase rapidly when the wide and narrow coal pillars are approximately 120 mm and 80 mm ahead of the mining face, respectively. From the above analysis, we deduced that decreasing the size of the coal pillars significantly decreases the convergence and the influence range.

To compare the advancement deformation range and the maximum convergence when retaining walls of different widths protect the coal pillars, we conducted a statistical analysis of the deformation behavior of the three test sites. The results of this analysis are shown in Figure 7. For wide coal pillars, the average maximum convergences of the

three test sites were approximately 730 mm, 918 mm, and 1110 mm, whereas the average maximum convergences of the three test sites were only 196 mm, 221 mm, and 247 mm for the narrow coal pillars. Furthermore, by comparing the ahead influence range of the different monitoring sites, we conclude that the advancement deformation ranges are approximately 84 m, 162 m, and 259 m for the 43 m wide coal pillars, while they are only 60.3 m, 104.3 m, and 147 m for the 8 m wide coal pillar. Although they all increase linearly, the increase rate of the narrow coal pillars is lower. In summary, when a narrow 8 m wide coal pillar is reserved, the cumulative convergence and the advancement deformation range are both smaller, and the adjacent gob-side entry is more stable.



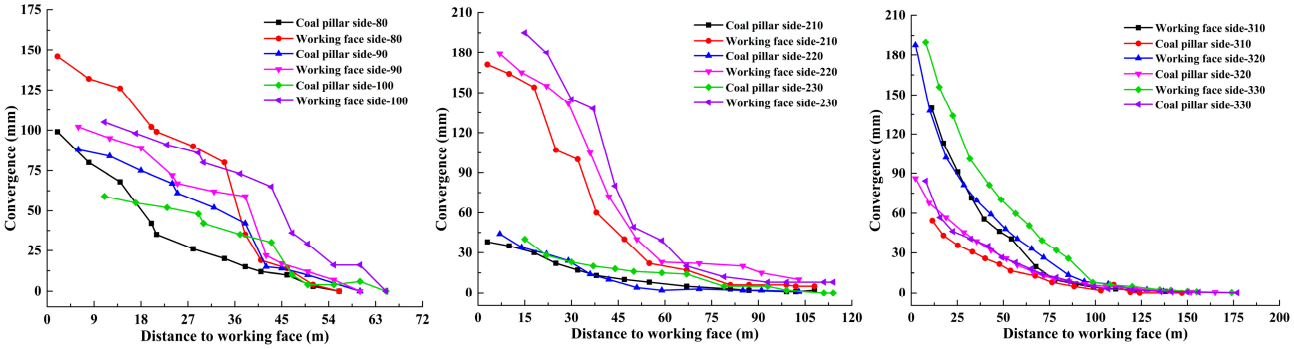

(**a**) Maximum convergence (**b**) Ahead range

**Figure 7.** Comparative analysis of the stability parameters at the three test sites.

### *4.3. Comparison of the Convergences of the Two Sides of the Roadway*

In addition, during the field investigation, we found that the convergence of the two walls of the roadway was non-uniform, and the convergence of the coal pillar side was significantly lower than that of the working face side when a concrete-consolidated coal pillar was present. To quantitatively compare and analyze the deformation of the ribs on both sides, we take sensor field III as an example. The results are shown in Figure 8. The average maximum convergences of the roadway ribs on the coal pillar side and the working face side were 75 mm and 172 mm, respectively. This is mainly because the reinforced coal pillar has a much greater stiffness than the working face, and coal pillars with smaller width-to-height ratios are prone to failure. Therefore, the reinforced concrete wall, which has a higher stiffness, hinders the lateral deformation of the narrow coal pillar and reduces rib convergence during the mining period.

The asymmetric rib convergence was closely related to the abutment pressure distribution around the gob-side entry. During the advance of the working face, the working-face side of the roadway was more directly affected by the front abutment pressure and mining-induced stress redistribution, resulting in relatively larger rib convergence. By contrast, the coal-pillar side was located adjacent to the gob, where partial stress relief occurred after mining. In addition, the reinforced concrete wall constructed along the coal pillar side provided lateral confinement and improved the bearing capacity of the coal pillar–roadway support system. Therefore, the coal-pillar-side convergence was smaller than the working-face-side convergence under the combined effects of abutment pressure distribution, gob-side stress relief, and concrete wall reinforcement.




(**a**) Field test site I (**b**) Field test site II (**c**) Field test site III

**Figure 8.** Comparison of the convergences of the two sides of the roadway in the presence of a concrete wall.

## 5. Deformation and Internal Fracture Zone Analysis

In order to compare and verify the application effect of establishing a small coal pillar in extra-thick coal seams, under the background of actual working conditions, field measurements were used to carry out research.

*Field Measurement Analysis of Internal Fracture*

The related technologies described in Section 3 were implemented in the roadway. The effects of their support are shown in Figure 9. Borehole television observations were used to investigate the internal fracture distribution of the narrow coal pillar. The results are shown in Figure 10.

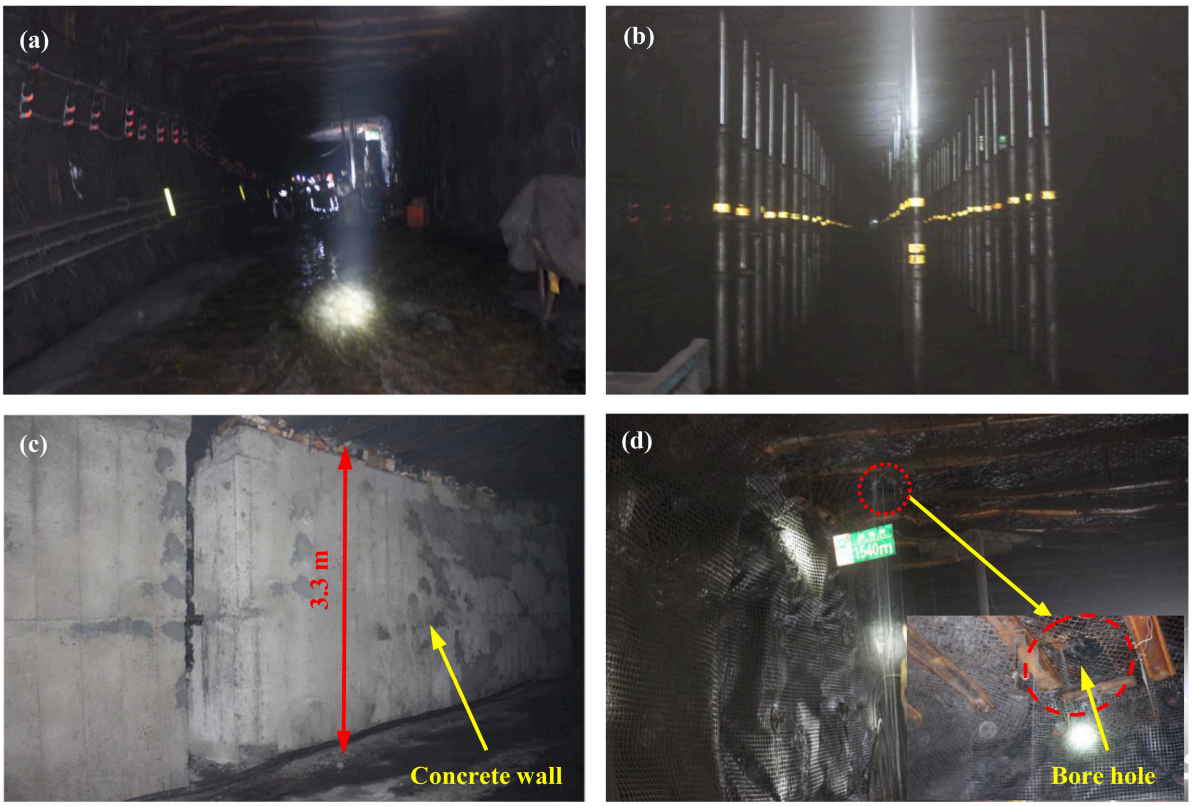



**Figure 9.** Effects of the roadway support in different stages. (**a**) roadway (**b**) roof (**c**) wall (**d**) hole.

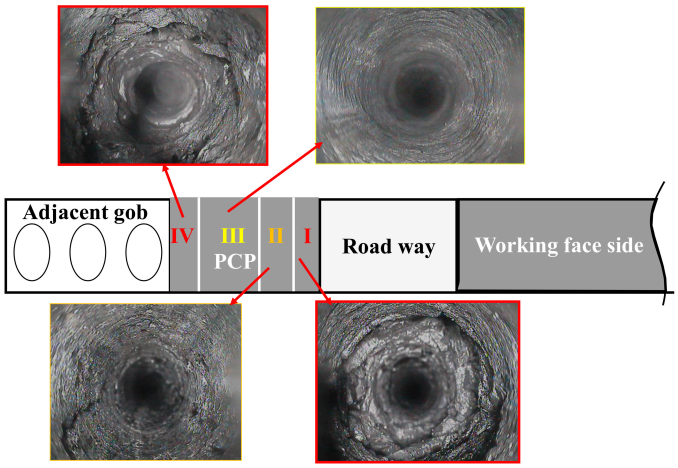



**Figure 10.** Camera detection and fracture zone distribution through the narrow coal pillar.

The surrounding rock deformation stabilized 10 days after the roadway excavation. Figure 9a shows that the rectangular roadway deformation is small and within the controllable range. There is no roof sagging, non-uniform sidewall spalling, or floor buckling. The overall effect of the support is good, indicating that the combined support method of anchors and cables can effectively control the deformation during excavation.

The reinforced concrete wall was constructed after the roadway deformation stabilized, and the mold was demolished after the wall had cured for 28 days. As shown in Figure 9c, the concrete wall remains perpendicular to the roof and floor and is very stable based on the on-site observations. There are no obvious cracks in or deformation of the concrete wall, which indicates that the concrete wall not only helps bear the weight of the overlying strata and reduces the roof sinking, but it also effectively prevents the narrow coal pillar's side rib from deforming into the roadway.

Directional hydraulic fracturing was also successfully implemented in the K3 sandstone. As the working face is rapidly advanced using high-strength mining, the hydraulic props at the front withstood the abutment stress, and the roadway was stable after the application of these methods.

In order to investigate the internal failure conditions, we used a borehole television optical imager to determine the fracture distribution throughout the narrow coal pillar. As shown in Figure 10, the coal pillar can be divided into four zones from the roadway to the gob based on the cracks in the surrounding rock. In zone I (0–1.5 m), the surrounding coal was broken, and criss-crossing fissures were present. In zone II (1.5 m to 2.5 m), the fracture distribution was smaller, and there was only one obvious longitudinal fissure. However, in zone III (2.5–6.5 m), the integrity was relatively good, and it was determined to be the most important area bearing the overlying load. In zone IV (6.5–8.0 m), the fractures were distributed near the gob, and the coal was broken, strongly criss-crossed with fissures, and hole collapse often occurred, which makes it like zone I.

Based on the above analysis, we conclude that the two sides (zones I and IV) of the narrow coal pillar were severely broken, but the inner part (zone III) had better integrity under the lateral disturbance loading. The pillar contains an elastic core zone with a certain width, which was the main zone bearing the overlying load and maintaining the coal pillar's stability under uniaxial compression. This demonstrates that a narrow 8 m wide coal pillar can not only ensure the stability of the roadway, but it also improves the resource recovery rate in extra-thick coal seam mining.

## 6. Discussion

Many interesting phenomena were found through the comparison and analysis of the convergence behaviour of the roadway when the width of the coal pillar was reduced. First, the results indicate that the deformation of the gob-side entry is much smaller when a concrete-reinforced, narrow, 8 m wide coal pillar is used in extra-thick coal seam mining than when a large 43 m wide coal pillar is used. Furthermore, the combination use of directional hydraulic fracturing of the roof and pouring concrete to consolidate the coal pillar decreased the deformation of the roadway of tailgate 8101. In general, there are two main reasons for the successful implementation of this on-site engineering trial. First, the reduction in the width of the coal pillar places the gob-side entry in a relatively low-stress environment, and the directional hydraulic fracturing of the roof prevents the transfer of the lateral stress in the key strata during mining. Second, the reinforcement provided by the high-strength reinforced concrete wall on the coal pillar side of the roadway results in the formation of a strong–weak coupled deformation joint structure, which can support the overlying load, so the roof sagging and the protrusion deformation of the roadway rib are reduced. Specifically, directional hydraulic fracturing was used to cut off or weaken the lateral stress transfer path of the overlying key strata, thereby creating a relatively low-stress environment around the gob-side entry. Meanwhile, the roadside concrete wall was used to reinforce the narrow coal pillar side, improve the lateral confinement and bearing capacity of the coal pillar–roadway support system, and control roadway rib convergence and roof subsidence. The simultaneous application of these two techniques forms a cooperative control mechanism of "roof pressure relief–coal pillar reinforcement–roadway deformation control", which is different from the separate use of either technique. The main innovation of this study is that it demonstrates the feasibility and effectiveness of this combined method for maintaining roadway stability when using an 8 m wide narrow coal pillar in a 17 m thick coal seam. This mining condition is characterized by high mining-induced stress, strong overlying strata movement, and a high risk of roadway deformation. Therefore, the proposed combined technology provides a new engineering approach for reducing coal pillar width, improving resource recovery, and ensuring roadway stability and mining safety in extra-thick coal seam mining.

The successful implementation of this field engineering trial can mainly be attributed to two aspects. First, from the perspective of mine pressure distribution, reducing the coal pillar width places the gob-side entry in a relatively low-stress environment. The larger 43 m wide coal pillar tends to accumulate higher abutment stress and may locate the roadway within an increased stress zone, resulting in more severe deformation of the surrounding rock during panel advancement. In contrast, the 8 m wide narrow coal pillar undergoes partial stress relief due to mining-induced stress redistribution, which helps reduce stress concentration near the roadway. Moreover, directional hydraulic fracturing of the roof can weaken the integrity of the key strata and prevent the transfer of lateral stress induced by overlying strata movement, thereby further improving the stress environment around the roadway. Secondly, the high-strength reinforced concrete wall constructed along the coal pillar side plays an important role in maintaining roadway stability. The concrete wall provides continuous lateral support, enhances the overall load-bearing capacity of the coal pillar–roadway support system, and restricts rib convergence and roof subsidence. In the case of the narrow coal pillar, the concrete wall works together with the coal pillar to form a strong–weak coupled deformation-bearing structure, which can effectively support the overlying load and control the deformation of the surrounding rock. Therefore, the combination of a narrow coal pillar, directional hydraulic roof fracturing, and concrete wall reinforcement creates a more favourable stress environment and significantly reduces roadway convergence.

In contrast, the larger 43 m wide coal pillar places the gob-side entry in the increased-stress zone, so the roadway deformation becomes more severe without effective measures, and slope expansion is needed to ensure normal recovery, which affects the recovery schedule, productivity, and safety of the mining operation. However, for rapid advancement and high-strength mining, when narrow coal pillars are used in combination with the roof fracturing and concrete reinforcement techniques, the convergence of the rock surrounding the roadway is small, indicating that the roadway remains highly stable. This ensures that normal production can progress, resulting in considerable economic benefits and increasing the average resource recovery rate by 3.6%. This technology improves the stress environment, reduces the deformation of the rock surrounding the roadway, and ensures the safety of the mine.

Reservoir stability is a prerequisite for the extraction of fossil fuels such as coal and oil [59–61]. The concrete wall filling along the coal pillar side is predicted to have a positive long-term effect on the stability of the roadway-surrounding rock [62–64]. By providing continuous lateral support, the concrete wall can effectively reduce the deformation of the coal pillar side, improve the stress transfer path, and alleviate stress concentration in the surrounding rock. This contributes to controlling roof subsidence, rib convergence, and potential instability of the roadway during the service period. From the perspective of mining safety, the improved long-term stability can reduce the probability of roof falling, rib spalling, and support system failure, thereby providing a safer working environment. These findings may offer guidance for the design of reinforced support systems in similar mining conditions and contribute to safer and more sustainable underground coal mining.

Although the combined use of reinforced concrete walls and directional hydraulic fracturing effectively controlled roadway deformation in this study, its field application requires additional cost, time, and construction organization. The concrete wall construction involves extra materials, equipment, labor, and curing time, while directional hydraulic fracturing requires drilling, sealing, high-pressure water injection equipment, and skilled operators. These measures may increase the initial investment and construction complexity, but they can reduce roadway maintenance, avoid repeated roadway enlargement, improve mining continuity, and enhance long-term safety. Some operational challenges should also be considered, including limited underground space, the accuracy of borehole positioning and fracturing direction, concrete pouring and curing quality, and coordination with the mining advance. Therefore, strict construction management and field monitoring are necessary during implementation. The applicability of this method may vary under different geological conditions. It is most suitable for extra-thick coal seams with strong mining-induced stress, large roadway deformation, and gob-side entry layouts. Before applying this technique to other mines, factors such as seam thickness, roof lithology, in situ stress level, coal pillar strength, groundwater conditions, and mining method should be carefully evaluated through site-specific analysis and field verification.

The field results of this study demonstrate that the observed improvement in roadway stability was achieved through the combined effect of the narrow coal pillar, directional hydraulic fracturing, and reinforced concrete wall. However, it should be noted that the present comparison between working face 8101 and working face 8106 involves multiple simultaneous variables, including pillar width, roof fracturing, and roadside reinforcement. Therefore, the present data do not allow the independent contribution of each measure to be quantified separately. In this sense, the conclusions of this study should be understood as reflecting the performance of the integrated control system rather than the effect of any single intervention. Future work should focus on isolating individual variables through additional field trials, laboratory tests, or numerical simulations to further clarify the specific role of each component in the overall control mechanism. It should be noted that this

study mainly focuses on the field monitoring response of the roadway-surrounding rock and the engineering effect of the combined control method. Some important mechanical parameters, such as the uniaxial compressive strength, tensile strength, fracture toughness of the key strata, in situ stress state, rock mass quality indices, mechanical properties of the coal seam, and cured compressive strength of the concrete wall, were not comprehensively analyzed in this study due to the limitations of the manuscript length and available test data. These parameters are important for quantitatively evaluating the mechanism of directional hydraulic fracturing and concrete wall reinforcement. Therefore, future studies should combine field monitoring with laboratory testing, in situ stress measurement, and mechanical modeling to further clarify the control mechanism and improve the reproducibility and applicability of the proposed method under different geological conditions. Nevertheless, to further promote the application of this technique, additional field trials should be conducted under similar geological and mining conditions. Moreover, theoretical modeling and laboratory tests are needed to further clarify the mechanical mechanism of the narrow coal pillar–concrete wall–roof fracturing cooperative control system [65,66]. These aspects will be investigated in our future work.

## 7. Conclusions

In this paper, we propose a longwall mining technique based on the use of a narrow coal pillar and a coal–concrete parallel retaining structure to prevent the deformation of the roadway. An industrial field test was carried out using a narrow 8 m coal pillar in the mining of an extra-thick coal seam. Roof directional hydraulic fracturing and the construction of a reinforced concrete wall beside the narrow coal pillar were implemented to improve the stability of the rock surrounding the gob-side entry. The roadway deformations for the 8 m and 43 m coal pillars were compared and comprehensively analyzed. The results indicate that the proposed technique is effective:

(1) The narrow coal pillar places the gob-side entry in a relatively low-stress environment and maintains its stability using several key techniques. The directional hydraulic fracturing of the roof inhibits the transfer of the local stress to the key roof strata, reduces the lateral abutment stress, and improves the roof's stability. Additionally, the reinforced concrete wall has greater stiffness than the coal, and thus, it can bear more of the load imposed by the overlying strata. It also reduces roof sinking and effectively prevents the lateral deformation of the coal pillar into the roadway.

(2) Through comparative analysis of the roadway convergences for the 43 m wide and 8 m wide coal pillars, we determined that the maximum convergence of the 8 m coal pillar during roadway excavation was only 41–61 mm, that is, about one-third of the convergence of the large coal pillar, and the time it took to reach stability after excavation was 10–13 d, that is, half of that for the 43 m coal pillar. The roadway convergence monitoring results collected while the working face was being mined also indicate that the maximum convergence and advancement influence range are all smaller for the 8 m coal pillar than for the 43 m coal pillar. Thus, the series of control measures implemented in this paper is effective, and the effect of the support provided by the 8 m coal pillar is significantly better than that provided by the 43 m coal pillar.

(3) When an 8 m wide coal pillar was used during mining, under the influence of mining stress, many cracks formed on both sides of the coal pillar, and the coal pillar was more broken on both sides, but there was a 4 m wide elastic core zone. This elastic core zone remained stable due to the additional support of the reinforced concrete wall, which ensured the safety of the mining operation. In addition, the proposed method significantly improves the resource recovery rate of extra-thick coal seam

mining. Thus, the research presented in this paper provides a reference for the mining of extra-thick coal seams under similar conditions.

**Author Contributions:** Conceptualization, C.Z.; Methodology, W.W. and C.Z.; Validation, T.D.; Formal analysis, W.Z.; Investigation, T.D. and Y.C.; Data curation, C.Z.; Writing—original draft, C.Z.; Visualization, W.Z.; Supervision, W.Z. All authors have read and agreed to the published version of the manuscript.

**Funding:** This work was supported by the National Natural Science Foundation of China (No. 52304149), the China Postdoctoral Science Foundation (No. 2024M760027), and the Anhui Province Postdoctoral Research Funding Project (No. 2025A1028).

**Data Availability Statement:** The original contributions presented in this study are included in the article. Further inquiries can be directed to the corresponding authors.

**Conflicts of Interest:** The authors Tao Ding, Chunwang Zhang were employed by the company Anhui Wanbei Coal-Electricity Group Co., Ltd. The author Wei Wang was employed by the company Datong Coal Mine Group Xuangang Coal-Electric Co., Ltd. The author Wenyang Zhang was employed by the company Jinneng Holding Shanxi Science and Technology Research Institute Co., Ltd. The author Yulong Chen was employed by the company Shanxi Coal Transportation and Sales Group Science and Technology Research Co., Ltd. The companies had no role in the design of the study; in the collection, analyses, or interpretation of data; in the writing of the manuscript, or in the decision to publish the results.

## References

1. He, M.C.; Wang, Q.; Wu, Q.Y. Innovation and future of mining rock mechanics. *J. Rock Mech. Geotech. Eng.* **2021**, *13*, 1–21. [CrossRef]
2. Liu, C.; Li, H.M.; Mitri, H.; Jiang, D.J.; Li, H.G.; Feng, J.F. Voussoir beam model for lower strong roof strata movement in longwall mining—Case study. *J. Rock Mech. Geotech. Eng.* **2017**, *9*, 1171–1176. [CrossRef]
3. Shen, W.; Bai, J.; Li, W.; Wang, X. Prediction of relative displacement for entry roof with weak plane under the effect of mining abutment stress. *Tunn. Undergr. Space Technol.* **2018**, *71*, 309–317. [CrossRef]
4. Zhao, T.B.; Guo, W.Y.; Tan, Y.L.; Yin, Y.C.; Cai, L.S.; Pan, J.F. Case Studies of Rock Bursts Under Complicated Geological Conditions During Multi-seam Mining at a Depth of 800 m. *Rock Mech. Rock Eng.* **2018**, *51*, 1539–1564. [CrossRef]
5. Hauquin, T.; Deck, O.; Gunzburger, Y. Average vertical stress on irregular elastic pillars estimated by a function of the relative extraction ratio. *Int. J. Rock Mech. Min. Sci.* **2016**, *83*, 122–134. [CrossRef]
6. Zhu, D.F.; Tu, S.H.; Tu, H.S.; Yang, Z.Q. Mechanisms of support failure and prevention measures under double-layer room mining gobs—A case study: Shigetai coal mine. *Int. J. Min. Sci. Technol.* **2019**, *29*, 955–962. [CrossRef]
7. Chen, S.J.; Wang, H.L.; Wang, H.Y.; Guo, W.J.; Li, X.S. Strip coal pillar design based on estimated surface subsidence in eastern China. *Rock Mech. Rock Eng.* **2016**, *49*, 3829–3838. [CrossRef]
8. Li, W.L.; Tu, S.H.; Tu, H.S.; Li, Y.; Liu, X.; Miao, K.J. Failure characteristics and control techniques for mining roadway affected by stress accumulation of residual pillars in contiguous coal seams. *Eng. Fail. Anal.* **2022**, *141*, 106646. [CrossRef]
9. Esterhuizen, G.S.; Gearhart, D.F.; Klemetti, T.; Dougherty, H.; Van Dyke, M. Analysis of gateroad stability at two longwall mines based on field monitoring results and numerical model analysis. *Int. J. Min. Sci. Technol.* **2019**, *29*, 35–43. [CrossRef]
10. Xie, H.P.; Gao, M.Z.; Zhang, R.; Peng, G.Y.; Wang, W.L.; Li, A.Q. Study on the Mechanical Properties and Mechanical Response of Coal Mining at 1000 m or Deeper. *Rock Mech. Rock Eng.* **2019**, *52*, 1475–1490. [CrossRef]
11. Zhang, C.W.; Jin, Z.X.; Song, X.M.; Feng, G.R.; Li, Z.; Gao, R.; Zhu, D.F.; Li, C. Failure mechanism and fracture aperture characteristics of hard thick main roof based on voussoir beam structure in longwall coal mining. *Energy Sci. Eng.* **2020**, *8*, 340–352. [CrossRef]
12. Yu, B.; Gao, R.; Kuang, T.J.; Huo, B.J.; Meng, X.B. Engineering study on fracturing high-level hard rock strata by ground hydraulic action. *Tunn. Undergr. Space Technol.* **2019**, *86*, 156–164. [CrossRef]
13. Zha, W.H.; Shi, H.; Liu, S.; Kang, C.H. Surrounding rock control of gob-side entry driving with narrow coal pillar and roadway side sealing technology in Yangliu Coal Mine. *Int. J. Min. Sci. Technol.* **2017**, *27*, 819–823. [CrossRef]
14. Lv, J.K.; Wan, Z.J.; Yang, Y.J.; Wang, Y.H.; Zhang, Y.; Liu, S.F. Failure characteristics and stability control technology of dynamic pressure roadway affected by the mining activity: A case study. *Eng. Fail. Anal.* **2022**, *131*, 105857. [CrossRef]
15. Li, G.J.; Wang, X.Y.; Bai, J.B.; Wu, B.W.; Wu, W.D. Research on the failure mechanism and control technology of surrounding rock in gob-side entry driving under unstable overlying strata. *Eng. Fail. Anal.* **2022**, *138*, 106361. [CrossRef]

16. Sinha, S.; Walton, G. Modeling behaviors of a coal pillar rib using the progressive S-shaped yield criterion. *J. Rock Mech. Geotech. Eng.* **2020**, *13*, 484–492. [CrossRef]
17. Yang, J.; Liu, C.; Yu, B.; Wu, F.F. Calculation and analysis of stress in strata under gob pillars. *J. Cent. South Univ.* **2015**, *22*, 1026–1036. [CrossRef]
18. Yang, Z.Q.; Liu, C.; Tang, S.C.; Dou, L.M.; Cao, J.L. Rock burst mechanism analysis in an advanced segment of gob-side entry under different dip angles of the seam and prevention technology. *Int. J. Min. Sci. Technol.* **2018**, *28*, 891–899. [CrossRef]
19. Kumar, A.; Kumar, D.; Singh, A.K.; Ram, S.; Kumar, R.; Gautam, A.; Singh, R.; Singh, A.K. Roof sagging limit in an early warning system for safe coal pillar extraction. *Int. J. Rock Mech. Min. Sci.* **2019**, *123*, 104131. [CrossRef]
20. Wang, H.W.; Xue, S.; Jiang, Y.D.; Deng, D.X.; Shi, S.Z.; Zhang, D.Q. Field investigation of a roof fall accident and large roadway deformation under geologically complex conditions in an underground coal mine. *Rock Mech. Rock Eng.* **2018**, *51*, 1863–1883. [CrossRef]
21. Young, M.; Walton, G.; Holley, E. Factors predictive of roof instability in addition to the existing CMRR criteria at two case study coal mines. *Int. J. Coal Geol.* **2019**, *213*, 103255. [CrossRef]
22. Deng, J.; Kanwar, N.S.; Pandey, M.D.; Xie, W.C. Dynamic buckling mechanism of pillar rockbursts induced by stress waves. *J. Rock Mech. Geotech. Eng.* **2019**, *11*, 944–953. [CrossRef]
23. Sun, H.; Liu, X.L.; Zhang, S.G.; Nawnit, K. Experimental investigation of acoustic emission and infrared radiation thermography of dynamic fracturing process of hard-rock pillar in extremely steep and thick coal seams. *Eng. Frac. Mech.* **2020**, *226*, 106845. [CrossRef]
24. Zhang, Q.; He, M.C.; Guo, S.; Qi, J.C.; Yang, J.; Wang, C.; Xia, M.; Li, L.N. Investigation on the key techniques and application of the new-generation automatically formed roadway without coal pillars by roof cutting. *Int. J. Rock Mech. Min. Sci.* **2022**, *152*, 105058. [CrossRef]
25. Cao, W.Z.; Shi, J.Q.; Si, G.Y.; Durucan, S.; Korre, A. Numerical modelling of microseismicity associated with longwall coal mining. *Int. J. Coal Geol.* **2018**, *193*, 30–45. [CrossRef]
26. Sinha, S.; Walton, G. Understanding continuum and discontinuum models of rock-support interaction for excavations undergoing stress-induced spalling. *Int. J. Rock Mech. Min. Sci.* **2019**, *123*, 104089. [CrossRef]
27. Bai, Q.S.; Tu, S.H.; Zhang, C.; Zhu, D.F. Discrete element modeling of progressive failure in a wide coal roadway from water-rich roofs. *Int. J. Coal Geol.* **2016**, *167*, 215–229. [CrossRef]
28. Wang, B.; Jiang, F.X.; Wang, C.; Zhang, B. Experimental study on the width of the reasonable segment pillar of the extremely soft coal seam in the deep mine. *Geotech. Geol. Eng.* **2019**, *37*, 4947–4957. [CrossRef]
29. Li, X.W.; Chai, Y.J. Determination of pillar width to improve mining safety in a deep burst- prone coal mine. *Saf. Sci.* **2019**, *113*, 244–256. [CrossRef]
30. Wu, W.D.; Bai, J.B.; Wang, X.Y.; Yan, S.; Wu, S.X. Numerical study of failure mechanisms and control techniques for a gob-side yield pillar in the Sijiazhuang coal mine, China. *Rock Mech. Rock Eng.* **2019**, *52*, 1231–1245. [CrossRef]
31. Zhang, P.; Gearhart, D.; Dyke, M.; Su, D.; Esterhuizen, E.; Tulu, B. Ground response to high horizontal stresses during longwall retreat and its implications for longwall headgate support. *Int. J. Min. Sci. Technol.* **2019**, *29*, 27–33. [CrossRef] [PubMed]
32. Yu, B.; Zhao, J.; Xiao, H.T. Case Study on Overburden Fracturing during Longwall Top Coal Caving Using Microseismic Monitoring. *Rock Mech. Rock Eng.* **2017**, *50*, 507–511. [CrossRef]
33. Zhang, Z.Y.; Zhang, N.; Shimada, H.; Sasaoka, T.; Wahyudi, S. Optimization of hard roof structure over retained goaf-side gateroad by pre-split blasting technology. *Int. J. Rock Mech. Min. Sci.* **2017**, *100*, 330–337. [CrossRef]
34. Kang, H.; Lv, H.; Gao, F.; Meng, X.; Feng, Y. Understanding mechanisms of destressing mining-induced stresses using hydraulic fracturing. *Int. J. Coal Geol.* **2018**, *196*, 19–28. [CrossRef]
35. Zhang, X.Y.; Pak, R.Y.S.; Gao, Y.B.; Liu, C.K.; Zhang, C.; Yang, J.; He, M.C. Field experiment on directional roof presplitting for pressure relief of retained roadways. *Int. J. Rock Mech. Min. Sci.* **2020**, *134*, 104436. [CrossRef]
36. Gao, Y.B.; Wang, Y.J.; Yang, J.; Zhang, X.Y.; He, M.C. Meso- and macro effects of roof split blasting on the stability of gateroad surroundings in an innovative nonpillar mining method. *Tunn. Undergr. Space Technol.* **2019**, *90*, 99–118. [CrossRef]
37. Wang, Q.; He, M.C.; Li, S.C.; Jiang, Z.H.; Wang, Y.; Qin, Q.; Jiang, B. Comparative study of model tests on automatically formed roadway and gob-side entry driving in deep coal mines. *Int. J. Min. Sci. Technol.* **2021**, *31*, 591–601. [CrossRef]
38. Wang, Y.J.; He, M.C.; Yang, J.; Wang, Q.; Liu, J.N.; Tian, X.C.; Gao, Y.B. Case study on pressure-relief mining technology without advance tunneling and coal pillars in longwall mining. *Tunn. Undergr. Space Technol.* **2020**, *97*, 103236. [CrossRef]
39. Wu, B.W.; Wang, X.Y.; Bai, J.B.; Wu, W.D.; Zhu, X.X.; Li, G.D. Study on crack evolution mechanism of roadside backfill body in gob- side entry retaining based on UDEC trigon model. *Rock Mech. Rock Eng.* **2019**, *52*, 3385–3399. [CrossRef]
40. Wang, Q.; He, M.C.; Yang, J.; Gao, H.K.; Jiang, B.; Yu, H.C. Study of a no-pillar mining technique with automatically formed gob-side entry retaining for longwall mining in coal mines. *Int. J. Rock Mech. Min. Sci.* **2018**, *110*, 1–8. [CrossRef]
41. Yang, J.; Fu, Q.; Gao, Y.B.; Wu, X.; Chang, X.; Li, C.J. A novel method of combined deep hole blasting for gob-side roadway protection. *Rock Mech. Rock Eng.* **2023**, *56*, 3551–3571. [CrossRef]

42. Lv, J.K.; Wan, Z.J.; Zhang, Y.; Wang, J.H.; Yan, W.Z.; Xiong, L.C. Effect of multi-factor dynamic loading on gob-side entry driving during longwall face extraction: A case study. *Bull. Eng. Geol. Environ.* **2022**, *81*, 409. [CrossRef]
43. Zhang, Z.Z.; Deng, M.; Wang, X.Y.; Yu, W.J.; Zhang, F.; Dao, V.D. Field and numerical investigations on the lower coal seam entry failure analysis under the remnant pillar. *Eng. Fail. Anal.* **2020**, *115*, 104638. [CrossRef]
44. Qiu, P.Q.; Ning, J.G.; Wang, J.; Hu, S.C.; Li, Z. Mitigating rock burst hazard in deep coal mines insight from dredging concentrated stress: A case study. *Tunn. Undergr. Space Technol.* **2021**, *115*, 104060. [CrossRef]
45. Xia, Z.; Yao, Q.L.; Meng, G.S.; Xu, Q.; Tang, C.J.; Zhu, L.; Wang, W.N.; Shen, Q. Numerical study of stability of mining roadways with 6.0-m section coal pillars under influence of repeated mining. *Int. J. Rock Mech. Min. Sci.* **2021**, *138*, 104641. [CrossRef]
46. Meng, N.K.; Bai, J.B.; Chen, Y.; Wang, X.Y.; Wu, W.D.; Wu, B.W. Stability analysis of roadside backfill body at gob-side entry retaining under combined static and dynamic loading. *Eng. Fail. Anal.* **2021**, *127*, 105531. [CrossRef]
47. Li, Z.L.; He, X.Q.; Dou, L.M.; Song, D.Z.; Wang, G.F. Numerical investigation of load shedding and rockburst reduction effects of top-coal caving mining in thick coal seams. *Int. J. Rock Mech. Min. Sci.* **2018**, *110*, 266–278. [CrossRef]
48. Ma, S.Q.; Chen, Y. Application of hydraulic fracturing and energy-absorption rockbolts to improve the stability of a gob-side roadway in a 10-m-thick coal seam: Case study. *Int. J. Geomech.* **2017**, *17*, 05017002. [CrossRef]
49. Tai, Y.; Xia, H.C.; Meng, X.B.; Kuang, F.J. Failure mechanism of the large-section roadway under mined zones in the ultra-thick coal seam and its control technology. *Energy Sci. Eng.* **2019**, *8*, 999–1014. [CrossRef]
50. Chen, Y.; Ma, S.Q.; Yu, Y. Stability control of underground roadways subjected to stresses caused by extraction of a 10-m-thick coal seam: A Case Study. *Rock Mech. Rock Eng.* **2017**, *50*, 2511–2520. [CrossRef]
51. Zhang, G.C.; Wen, Z.J.; Liang, S.J.; Tan, Y.L.; Tian, L.; Zhao, Y.Q.; Zhao, D.S. Ground response of a gob-side entry in a longwall panel extracting 17 m-thick coal seam: A Case Study. *Rock Mech. Rock Eng.* **2020**, *53*, 497–516. [CrossRef]
52. Wang, H.S.; Wang, J.; Elmo, D.; He, M.C.; Ma, Z.M.; Gao, C.Z. Ground response mechanism of entries and control methods induced by hard roof in longwall top coal caving panel. *Eng. Fail. Anal.* **2023**, *144*, 106940. [CrossRef]
53. Gao, R.; Yu, B.; Meng, X.B. Stress distribution and surrounding rock control of mining near to the overlying coal pillar in the working face. *Int. J. Min. Sci. Technol.* **2019**, *29*, 881–887. [CrossRef]
54. Li, Z.; Xu, J.L.; Ju, J.F.; Zhu, W.B.; Xu, J.M. The effects of the rotational speed of voussoir beam structures formed by key strata on the ground pressure of stopes. *Int. J. Rock Mech. Min. Sci.* **2018**, *108*, 67–79. [CrossRef]
55. Li, Z.; Yu, S.C.; Zhu, W.B.; Feng, G.R.; Xu, J.M.; Guo, Y.X.; Qi, T.Y. Dynamic loading induced by the instability of voussoir beam structure during mining below the slope. *Int. J. Rock Mech. Min. Sci.* **2020**, *132*, 104343. [CrossRef]
56. Wen, Z.J.; Xing, E.R.; Shi, S.; Jiang, Y.J. Overlying strata structural modeling and support applicability analysis for large mining-height stopes. *J. Loss Prev. Process Ind.* **2019**, *57*, 94–100. [CrossRef]
57. Zhao, Y.H.; Wang, S.R.; Zou, Z.S.; Ge, L.L.; Cui, F. Instability characteristics of the cracked roof rock beam under shallow mining conditions. *Int. J. Min. Sci. Technol.* **2018**, *28*, 437–444. [CrossRef]
58. Zhu, W.B.; Chen, L.; Zhou, Z.L.; Shen, B.T.; Xu, Y. Failure Propagation of Pillars and Roof in a Room and Pillar Mine Induced by Longwall Mining in the Lower Seam. *Rock Mech. Rock Eng.* **2019**, *52*, 1193–1209. [CrossRef]
59. Li, Q.; Li, Q.; Wang, F.; Wu, J.; Wang, Y.; Jin, J. Effects of geological and fluid characteristics on the injection filtration of hydraulic fracturing fluid in the wellbores of shale reservoirs: Numerical analysis and mechanism determination. *Processes* **2025**, *13*, 1747. [CrossRef]
60. Li, Q.; You, D.; Li, Q.; Wang, F.; Wang, Y.; Yang, Y. Analysis of sedimentation behavior and influencing factors of solid particles in $CO_2$ fracturing fluid. *Processes* **2025**, *13*, 4049. [CrossRef]
61. Li, Y.; Yang, J.; Yu, Q.; Liu, X.; Guo, W.; Miao, S. 3D coupled dynamic modeling of deep shaft excavation near a fault: Coseismic slip and seismic hazards. *J. Rock Mech. Geotech. Eng.* 2025; *in press*. [CrossRef]
62. Li, Y. Spatial distribution of strain energy changes due to mining-induced fault coseismic slip: Insights from a rockburst at the Yuejin coal mine, China. *Rock Mech. Rock Eng.* **2025**, *58*, 1693–1706. [CrossRef]
63. Li, Y.; Yang, J.; Gao, X. Fault slip amplification mechanisms in deep mining due to heterogeneous geological layers. *Eng. Fail. Anal.* **2025**, *169*, 109155.
64. Li, Y.; Fukuyama, E.; Yoshimitsu, N. Comprehensive 3-D modeling of mining-induced fault slip: Impact of panel length, panel orientation and far-field stress orientation. *Rock Mech. Rock Eng.* **2025**, *58*, 5961–5979. [CrossRef]
65. Li, Q.; Li, Q.; Wu, J.; He, K.; Xia, Y.; Liu, J.; Wang, F.; Cheng, Y. Wellhead Stability During Development Process of Hydrate Reservoir in the Northern South China Sea: Sensitivity Analysis. *Processes* **2025**, *13*, 1630. [CrossRef]
66. Li, Y.; Gao, X. Assessment of variations in shear strain energy induced by fault coseismic slip in deep longwall mining. *Int. J. Coal Sci. Technol.* **2025**, *12*, 3–16. [CrossRef]


**Disclaimer/Publisher's Note:** The statements, opinions and data contained in all publications are solely those of the individual author(s) and contributor(s) and not of MDPI and/or the editor(s). MDPI and/or the editor(s) disclaim responsibility for any injury to people or property resulting from any ideas, methods, instructions or products referred to in the content.